Atmos. Chem. Phys., 16, 14463–14474, 2016
www.atmos-chem-phys.net/16/14463/2016/
doi:10.5194/acp-16-14463-2016

Atmospheric Chemistry and Physics Open Access EGU

Ozone production and its sensitivity to NO_x and VOCs: results from the DISCOVER-AQ field experiment, Houston 2013

Gina M. Mazzuca[1], Xinrong Ren[1,2], Christopher P. Loughner[2,3], Mark Estes[4], James H. Crawford[5], Kenneth E. Pickering[1,6], Andrew J. Weinheimer[7], and Russell R. Dickerson[1]

[1]Department of Atmospheric and Oceanic Science, University of Maryland, College Park, MD 20742, USA
[2]Air Resources Laboratory, National Oceanic and Atmospheric Administration, College Park, MD 20740, USA
[3]Earth System Science Interdisciplinary Center, University of Maryland, College Park, MD 20740, USA
[4]Texas Commission on Environmental Quality, Austin, TX 78711, USA
[5]NASA Langley Research Center, Hampton, VA 23681, USA
[6]NASA Goddard Space Flight Center, Greenbelt, MD 20771, USA
[7]National Center for Atmospheric Research, Boulder, CO 80307, USA

Correspondence to: Xinrong Ren (ren@umd.edu)

Received: 11 March 2016 – Published in Atmos. Chem. Phys. Discuss.: 13 May 2016
Revised: 22 August 2016 – Accepted: 11 October 2016 – Published: 22 November 2016

Abstract. An observation-constrained box model based on the Carbon Bond mechanism, version 5 (CB05), was used to study photochemical processes along the NASA P-3B flight track and spirals over eight surface sites during the September 2013 Houston, Texas deployment of the NASA Deriving Information on Surface Conditions from COlumn and VERtically Resolved Observations Relevant to Air Quality (DISCOVER-AQ) campaign. Data from this campaign provided an opportunity to examine and improve our understanding of atmospheric photochemical oxidation processes related to the formation of secondary air pollutants such as ozone (O_3). O_3 production and its sensitivity to NO_x and volatile organic compounds (VOCs) were calculated at different locations and times of day. Ozone production efficiency (OPE), defined as the ratio of the ozone production rate to the NO_x oxidation rate, was calculated using the observations and the simulation results of the box and Community Multiscale Air Quality (CMAQ) models. Correlations of these results with other parameters, such as radical sources and NO_x mixing ratio, were also evaluated. It was generally found that O_3 production tends to be more VOC-sensitive in the morning along with high ozone production rates, suggesting that control of VOCs may be an effective way to control O_3 in Houston. In the afternoon, O_3 production was found to be mainly NO_x-sensitive with some exceptions. O_3 production near major emissions sources such as Deer Park was mostly VOC-sensitive for the entire day, other urban areas near Moody Tower and Channelview were VOC-sensitive or in the transition regime, and areas farther from downtown Houston such as Smith Point and Conroe were mostly NO_x-sensitive for the entire day. It was also found that the control of NO_x emissions has reduced O_3 concentrations over Houston but has led to larger OPE values. The results from this work strengthen our understanding of O_3 production; they indicate that controlling NO_x emissions will provide air quality benefits over the greater Houston metropolitan area in the long run, but in selected areas controlling VOC emissions will also be beneficial.

1 Introduction

Understanding the nonlinear relationship between ozone production and its precursors is critical for the development of an effective ozone (O_3) control strategy. Despite great efforts undertaken in the past decades to address the problem of high ozone concentrations, our understanding of the key precursors that control tropospheric ozone production remains incomplete and uncertain (Molina and Molina, 2004; Xue et al., 2013). Atmospheric ozone levels are determined by emissions of ozone precursors, atmospheric photochemistry, and transport (Jacob, 1999; Xue et al., 2013). A major challenge

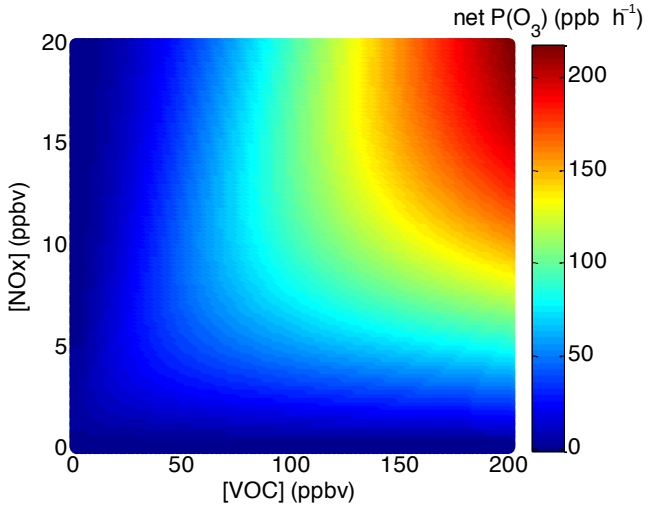

Figure 1. Ozone production empirical kinetic modeling approach (EKMA) diagram using box model results with NOx levels varying from 0 to 20 ppbv and VOC levels from 0 to 200 ppbv. The mean concentrations of other species and the speciation of NO_x and VOCs observed during DISCOVER-AQ in Houston in 2013 were used to constrain the box model. This diagram clearly shows the sensitivity of ozone production to NO_x and VOCs in Houston.

in regulating ozone pollution lies in comprehending its complex and nonlinear chemistry with respect to ozone precursors, i.e., nitrogen oxides (NO_x) and volatile organic compounds (VOCs), that varies with time and location (Fig. 1). Understanding the nonlinear relationship between ozone production and its precursors is critical for the development of an effective ozone control strategy.

Sensitivity of ozone production to NO_x and VOCs represents a major uncertainty for oxidant photochemistry in urban areas (Sillman et al., 1995, 2003). In urban environments, ozone is formed through photochemical processes when its precursors NO_x and VOCs are emitted into the atmosphere from many sources. Depending on physical and chemical conditions, the production of ozone can be either NO_x-sensitive or VOC-sensitive due to the complexity of these photochemical processes. Therefore, effective ozone control strategies rely heavily on the accurate understanding of how ozone responds to reduction of NO_x and VOC emissions, usually simulated by photochemical air quality models (e.g., Sillman et al., 2003; Lei et al., 2004; Mallet and Sportisse, 2005; Li et al, 2007; Chen et al., 2010; Tang et al., 2010; Xue et al., 2013; Goldberg et al., 2016). However, those model-based studies have inputs or parameters subject to large uncertainties that can affect not only the simulated levels of ozone but also the ozone dependence on its precursors.

There are some observation-based studies of ozone production and its relationships with NO_x and VOCs (e.g., Thielmann et al., 2002; Zaveri et al., 2003; Ryerson et al., 2003; Griffin et al., 2003; Kleinman et al., 2005a; Neuman et al., 2009; Mao et al., 2010; Ren et al., 2013). Using in situ aircraft observations, Kleinman et al. (2005a) studied five US cities and found that ozone production rates vary from nearly 0 to 155 ppbv h^{-1}, with differences depending on the concentration of ozone precursors NO_x and VOCs. They also found that, in Houston, NO_x and light olefins are co-emitted from petrochemical facilities, leading to the highest ozone production of the five cities (Kleinman et al., 2005a). Using the data collected at a single surface location during the Study of Houston Atmospheric Radical Precursors (SHARP) in spring 2009, the temporal variation of O_3 production was observed: VOC-sensitive in the early morning and NO_x-sensitive for most of the afternoon (Ren et al., 2013). This is similar to the behavior observed in two previous summertime studies in Houston: the Texas Air Quality Study in 2000 (TexAQS 2000) and the TexAQS II Radical and Aerosol Measurement Project in 2006 (TRAMP 2006) (Mao et al., 2010; Chen et al., 2010). In a more recent study using measurements in four cities in China, ozone production was found to be in a VOC-sensitive regime in both Shanghai and Guangzhou but in a mixed regime in Lanzhou (Xue et al., 2013). In the work presented here, we provide investigations of spatial and temporal variations of ozone production and its sensitivity to NO_x and VOCs to provide a scientific basis to develop a non-uniform emission reduction strategy for O_3 pollution control in urban and suburban areas such as the greater Houston metropolitan area.

This work utilized observations made during the Deriving Information on Surface Conditions from COlumn and VERtically Resolved Observations Relevant to Air Quality (DISCOVER-AQ) campaign in Houston in September 2013. This field campaign is unique due to the comprehensive air sampling performed over a large spatial (urban and suburban areas in and around Houston) and temporal (entire month of September 2013) range. Measurements were collected from various platforms including the National Aeronautics and Space Administration (NASA) P-3B and B-200 aircraft, ground surface sites, and mobile laboratories. Eight surface monitoring stations (Smith Point, Galveston, Manvel Croix, Deer Park, Channelview, Conroe, West Houston, and Moody Tower) were selected where the P-3B conducted vertical spirals (Fig. 2) (DISCOVER-AQ whitepaper, 2009).

2 Methods

2.1 Ozone production scenarios and sensitivity

During the day, the photochemical O_3 production rate is essentially the production rate of NO_2 molecules from $HO_2 + NO$ and $RO_2 + NO$ reactions (Finlayson-Pitts and Pitts, 2000). The net instantaneous photochemical O_3 production rate, $P(O_3)$, can be written approximately as the following equation:

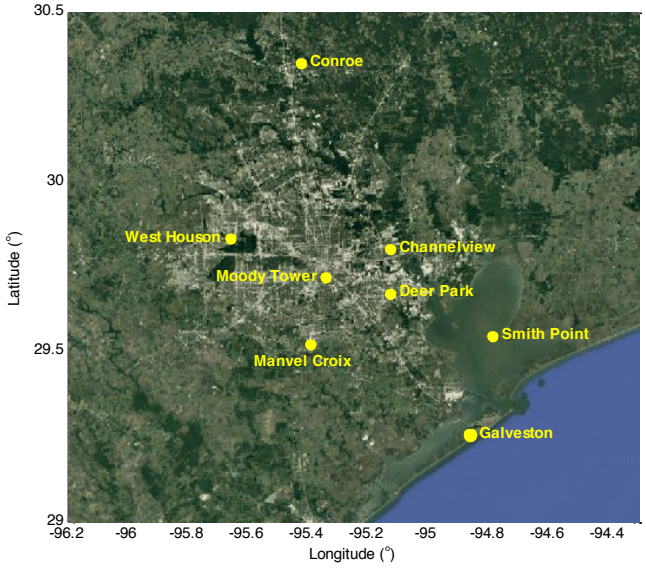

Figure 2. DISCOVER-AQ ground and spiral sites (yellow dots) during the September 2013 Houston campaign.

$$P(O_3) = k_{HO_2+NO}[HO_2][NO] + \sum k_{RO_{2i}+NO}[RO_{2i}][NO] - k_{OH+NO_2+M}[OH][NO_2][M] - P(RONO_2) - k_{HO_2+O_3}[HO_2][O_3] - k_{OH+O_3}[OH][O_3] - k_{O(^1D)+H_2O}[O(1D)][H_2O] - L(O_3 + \text{alkenes}), \quad (1)$$

where k terms are the reaction rate coefficients; RO_{2i} is the individual organic peroxy radicals. The negative terms in Eq. (1) correspond to the reaction of OH and NO_2 to form nitric acid, the formation of organic nitrates, $P(RONO_2)$, the reactions of OH and HO_2 with O_3, the photolysis of O_3 followed by the reaction of $O(^1D)$ with H_2O, and O_3 reactions with alkenes. Ozone is additionally destroyed by dry deposition.

The dependence of O_3 production on NO_x and VOCs can be categorized into two typical scenarios: NO_x-sensitive and VOC-sensitive. The method proposed by Kleinman (2005b) was used to evaluate the O_3 production sensitivity using the ratio of L_N/Q, where L_N is the radical loss via the reactions with NO_x and Q is the total primary radical production. Because the radical production rate is approximately equal to the radical loss rate, this L_N/Q ratio represents the fraction of radical loss due to NO_x. It was found that, when L_N/Q is significantly less than 0.5, the atmosphere is in a NO_x-sensitive regime and that, when L_N/Q is significantly greater than 0.5, the atmosphere is in a more VOC-sensitive regime (Kleinman et al., 2001, 2005b). Note that the contribution of organic nitrates impacts the cutoff value for L_N/Q to determine the ozone production sensitivity to NO_x or VOCs, and this value may vary slightly around 0.5 in different environments (Kleinman, 2005b).

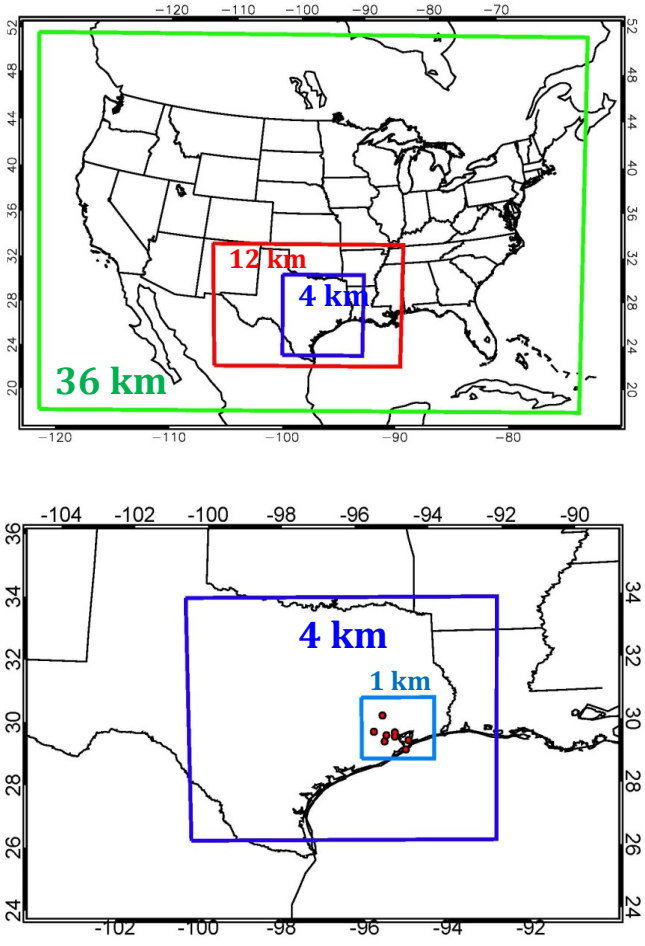

Figure 3. 36, 12, and 4 km CMAQ modeling domains (top); 4 and 1 km CMAQ modeling domains. The red dots show the NASA P-3B aircraft spiral locations (bottom).

2.2 Box model simulations

An observation-constrained box model with the Carbon Bond Mechanism, version 5 (CB05), was used to simulate the oxidation processes in Houston during DISCOVER-AQ. Measurements made on the P-3B were used as input to constrain the box model. From the box model results, the ozone production rate and its sensitivity to NO_x and VOCs were calculated, allowing us to calculate ozone production efficiency at different locations and at different times of day.

CB05 is a well-known chemical mechanism that has been actively used in research and regulatory applications (Yarwood et al., 2005). Organic species are lumped according to the carbon bond approach, that is, bond type, e.g., carbon single bond and double bond. Reactions are aggregated based on the similarity of carbon bond structure so that fewer surrogate species are needed in the model. Some organics (e.g., organic nitrates and aromatics) are lumped together. The lifetime of alkyl nitrates is too long in CB05 and has been corrected in CB6r2 (Canty et al., 2015), but this should

Table 1. WRF and CMAQ model options that were used in both the original and improved modeling scenarios.

Weather Research and Forecasting (WRF) version 3.6.1 model options	
Radiation	Longwave: Rapid Radiative Transfer Model (RRTM) Shortwave: Goddard
Surface layer	Pleim-Xiu
Land surface model	Pleim-Xiu
Boundary layer	Asymmetric Convective Model (ACM2)
Cumulus	Kain-Fritsch
Microphysics	WRF Single-Moment 6 (WSM-6)
Nudging	Observational and analysis nudging
Damping	Vertical velocity and gravity waves damped at top of modeling domain
SSTs	Multi-scale Ultra-high Resolution (MUR) SST analysis ($\sim$ 1 km resolution)
Meteorological initial and boundary conditions and analysis nudging inputs	NAM 12 km
Observational nudging inputs	NCEP ADP Global Surface and Upper Air Observational Weather Data
CMAQ version 5.0.2 model options	
Chemical mechanism	Carbon Bond mechanism (CB05)
Aerosol module	Aerosols with aqueous extensions version 5 (AE5)
Dry deposition	M3DRY
Vertical diffusion	Asymmetric Convective Model 2 (ACM2)
Emissions	2012 TCEQ anthropogenic emissions Biogenic Emission Inventory System (BEIS) calculated within CMAQ
Chemical initial and boundary conditions	Model for OZone and Related chemical Tracers (MOZART) chemical transport model (CTM)

have minimal impact on our findings because the model is constrained to observations as indicated below.

The box model was run using measurements, including long-lived inorganic and organic compounds and meteorological parameters (temperature, pressure, humidity, and photolysis frequencies), from the NASA P-3B. One-minute archived data were used as model input (available at http://www-air.larc.nasa.gov/missions/discover-aq/discover-aq.html). The model ran for 24 h for each data point to allow most calculated reactive intermediates to reach steady state but short enough to prevent the buildup of secondary products. An additional lifetime of 2 days was assumed for some calculated long-lived species, such as organic acids and alcohols, to avoid unexpected accumulation of these species in the model. At the end of 24 h, the model generated time series of OH, HO_2, RO_2, and other reactive intermediates. The box model simulations covered the entire P-3B flight track during DISCOVER-AQ, including the eight science sites where the P-3B conducted spirals. Note that unlike a three-dimensional chemical transport model the zero-dimensional box model simulations did not include advection and emissions. Although advection and emissions are certainly important factors for the air pollution formation, they can be omitted in the box model since all of the long-lived radical and O_3 precursors were measured and used to constrain the box model calculations. The box model analysis is necessary for ozone production and its sensitivity to NO_x and VOCs because the box model was constrained to measured species (e.g., NO, NO_2, CO, HCHO) and meteorological parameters (e.g., photolysis frequencies) that are essential to calculate ozone production rates. Even though there is good agreement in general between the box model and the 3-D model, there are still some differences between the measurements and the output from the 3-D model that are shown below, e.g., NO_x, CO, HCHO, and photolysis frequencies.

2.3 WRF–CMAQ model simulations

The Weather Research and Forecasting (WRF) model was run from 18 August 2013 to 1 October 2013 with nested domains with horizontal resolutions of 36, 12, 4, and 1 km and 45 vertical levels. This work utilized results from the 4 km domain. The modeling domains are shown in Fig. 3. WRF was run straight through (i.e., was not re-initialized at all) using an iterative technique developed at the EPA and de-

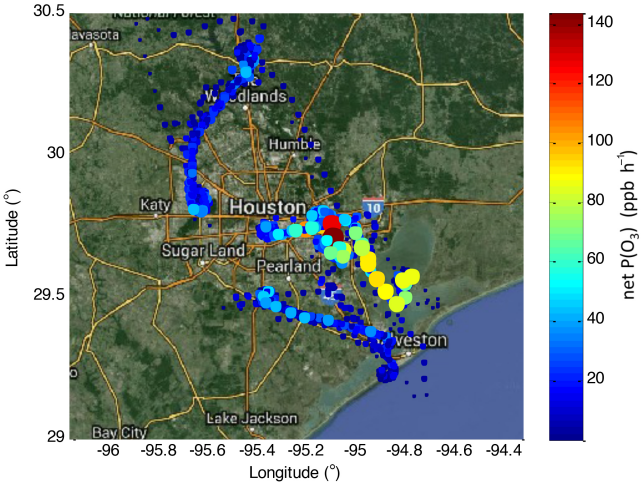

Figure 4. Net ozone production rate, net $P(O_3)$, calculated using the box model results along the P-3B flight track during DISCOVER-AQ in Houston in 2013. The size of dots is proportional to $P(O_3)$.

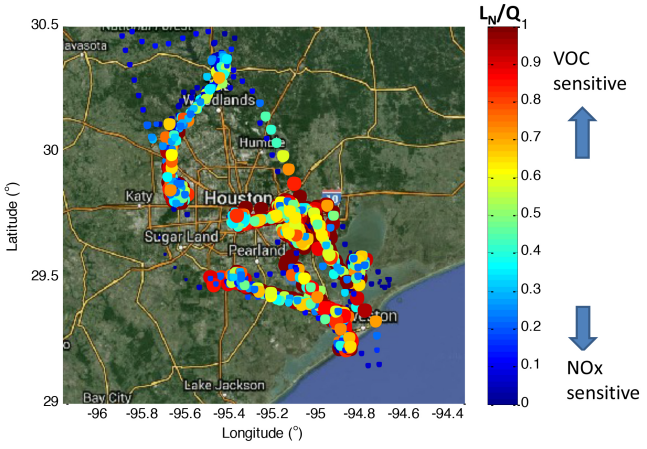

Figure 5. Ozone production sensitivity indicator, L_N/Q, along the P-3B flight track during DISCOVER-AQ in Houston in 2013. $P(O_3)$ is VOC-sensitive when $L_N/Q > 0.5$ and NO_x-sensitive when $L_N/Q < 0.5$.

scribed in Appel et al. (2014). Observational and analysis nudging were performed on all domains. Model output was saved hourly for the 36 and 12 km domains, every 20 min for the 4 km domain, and every 5 min for the 1 km domain. WRF and Community Multiscale Air Quality (CMAQ) configuration options and inputs are shown in Table 1.

WRF model results were used to drive the CMAQ model offline. The 2012 baseline anthropogenic emissions from the Texas Commission on Environmental Quality (TCEQ) were used as input to CMAQ. These emissions contain the most-up-to-date Texas anthropogenic emissions inventory and a compilation of emissions estimates from regional planning offices throughout the US. Biogenic emissions were calculated online within CMAQ with the Biogenic Emission Inventory System (BEIS). Lightning emissions were also calculated online within CMAQ. CMAQ was run with the process analysis tool to output ozone production rate ($P(O_3)$), ozone loss rate ($L(O_3)$), and net ozone production rate (net $P(O_3)$) as well as OPE.

3 Results

3.1 Photochemical O_3 production rate, sensitivity, and diurnal variations

Figure 4 shows the net $P(O_3)$ calculated using the box model results along the P-3B flight track for all flight days during the Houston deployment. There are several $P(O_3)$ hot spots over the Houston Ship Channel located to the east/southeast of downtown Houston as well as downwind, over Galveston Bay. This is expected because of large emissions of NO_x and VOCs from the Houston Ship Channel, where the highest $P(O_3)$ was observed – up to ~ 140 ppbv h^{-1}. $P(O_3)$ values up to $\sim$ 80-90 ppbv h^{-1} were observed over Galveston Bay, mainly on 25 September 2013, consistent with high ozone levels observed across the Houston area on that day. Similar instantaneous ozone production rates have been observed in two previous studies in Houston in 2000 and 2006 (Kleinman et al., 2002; Mao et al., 2010).

Figure 5 shows the indicator L_N/Q of ozone production sensitivity along the P-3B flight track for all flight days during the Houston deployment. $P(O_3)$ was mainly VOC-sensitive over the Houston Ship Channel and its surrounding urban areas due to large NO_x emissions. Over areas away from the center of the city with relatively low NO_x emissions, $P(O_3)$ was usually NO_x-sensitive. Vertical profiles of $P(O_3)$, $L(O_3)$, and net ozone production calculated using the box model results (Fig. 6) show that

1. $RO_2 + NO$ makes about the same amount of O_3 as $HO_2 + NO$ in the model,
2. O_3 photolysis followed by $O(^1D) + H_2O$ is a dominant process for the photochemical ozone loss,
3. the maximum net $P(O_3)$ appeared near the surface below 1 km.

In the diurnal variations of $P(O_3)$, a broad peak in the morning with significant $P(O_3)$ in the afternoon was obtained on 10 flight days during DISCOVER-AQ in Houston (Fig. 7). High $P(O_3)$ mainly occurred with $L_N/Q > 0.5$ (i.e., in the VOC-sensitive regime). The diurnal variation of L_N/Q indicates that $P(O_3)$ was mainly VOC-sensitive in the early morning and then transitioned towards the NO_x-sensitive regime later in the day (Fig. 8). High $P(O_3)$ in the morning was mainly associated with VOC sensitivity due to high NO_x levels in the morning (points in the red circle in Fig. 8). Although $P(O_3)$ was mainly NO_x-sensitive in the

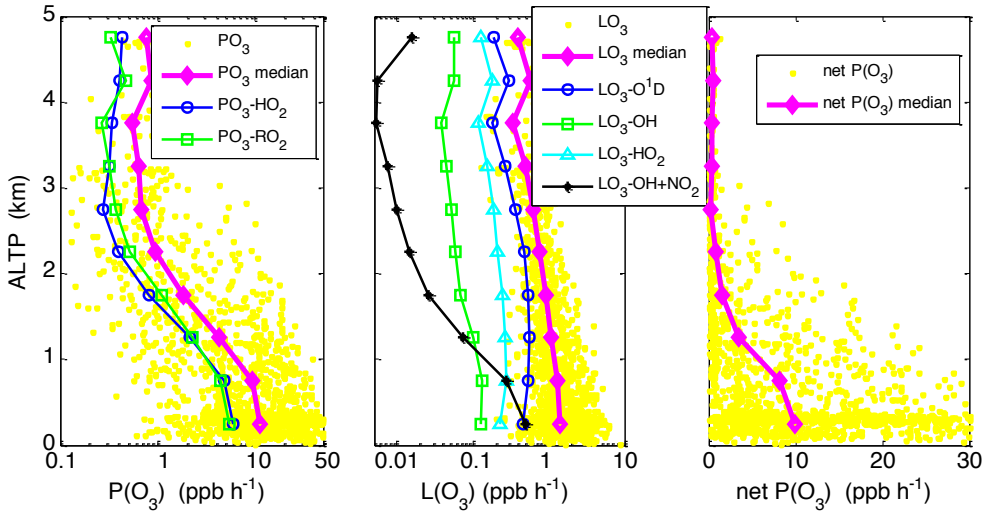

Figure 6. Vertical profiles of ozone production rate (left), ozone loss rate (middle), and net ozone production rate (right) during DISCOVER-AQ in Houston in 2013.

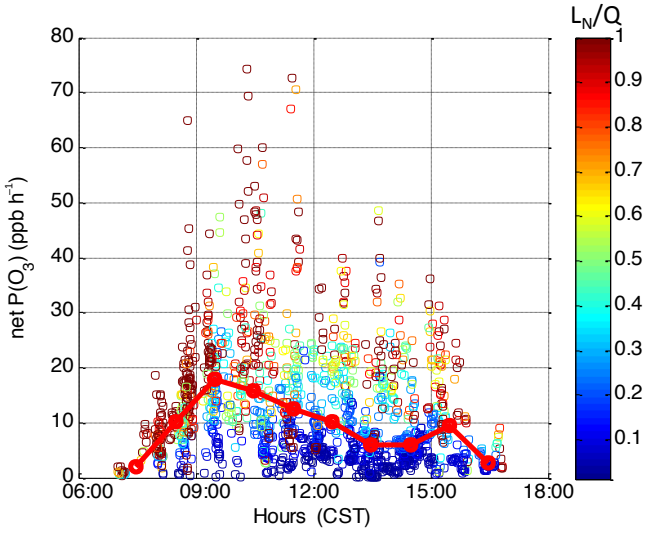

Figure 7. Diurnal variation of ozone production rate colored with the indicator L_N/Q on 10 flight days during DISCOVER-AQ in Houston in 2013. The solid red circles represent the median values in hourly bins of $P(O_3)$. Data are limited with the pressure altitude less than 1000 m to represent the lowest layer of the atmosphere.

afternoon between 12:00 and 17:00 Central Standard Time (CST: UTC−6 h), there were also periods and locations when $P(O_3)$ was VOC-sensitive, e.g., the points with $L_N/Q > 0.5$ between 12:00 and 17:00 CST in Fig. 8.

Diurnal variations of ozone production rate at eight individual locations where the P-3B conducted vertical spirals show that the ozone production is greater than 10 ppbv h^{-1} on average at locations with high NO_x and VOC emissions, such as Deer Park, Moody Tower, and Channelview, while at locations away from the urban center with lower emissions – such as Galveston, Smith Point, and Conroe – the ozone production usually averaged less than 10 ppbv h^{-1} (Fig. 9). The dependence of $P(O_3)$ on the NO mixing ratio ([NO]) shows that, when [NO] is less than ∼1 ppbv, ozone production increases as the [NO] increases; i.e., $P(O_3)$ is in a NO_x-sensitive regime. When the NO mixing ratio is greater than ∼1 ppbv, ozone production levels off; i.e., $P(O_3)$ is in a NO_x-saturated regime (Fig. 10). It was also found that at a given NO mixing ratio a higher production rate of HO_x results in a higher ozone production rate. Diurnal variations of the indicator of ozone production sensitivity to NO_x and VOCs, L_N/Q, at eight individual locations where the P-3B conducted vertical spirals show that (1) at Deer Park $P(O_3)$ was mostly VOC-sensitive for the entire day; (2) at Moody Tower and Channelview $P(O_3)$ was VOC-sensitive or in the transition regime; (3) at Smith Point and Conroe $P(O_3)$ was mostly NO_x-sensitive for the entire day; and (4) at Galveston, West Houston, and Manvel Croix $P(O_3)$ was VOC sensitive only in the early morning (Fig. 11).

3.2 Ozone production efficiency

OPE is defined as the number of molecules of oxidant O_x ($= O_3 + NO_2$) produced photochemically when a molecule of NO_x ($= NO + NO_2$) is oxidized. It conveys information about the conditions under which O_3 is formed and is an important parameter to consider when evaluating impacts from NO_x emission sources (Kleinman et al., 2002). The OPE can be deduced from atmospheric observations as the slope of a graph of O_x concentration vs. the concentration of NO_x oxidation products. The latter quantity is denoted as NO_z and is commonly measured as the difference between NO_y (sum of all reactive-nitrogen compounds) and NO_x, i.e., $NO_z = NO_y - NO_x$.

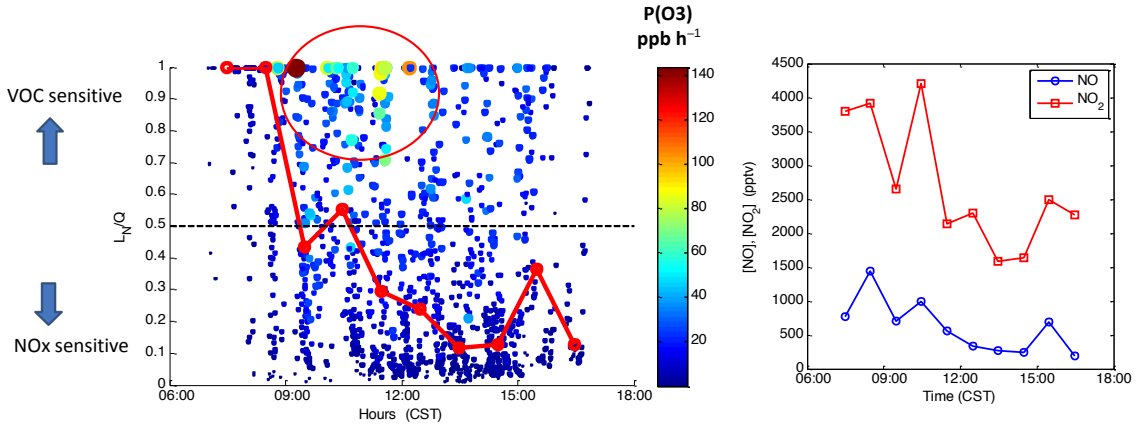

Figure 8. Diurnal variations of the indicator L_N/Q of ozone production rate sensitivity colored with ozone production rate and median hourly bins of L_N/Q shown in solid red circles (left) and median hourly NO and NO_2 concentrations (right) below 1000 m during DISCOVER-AQ in Houston in 2013.

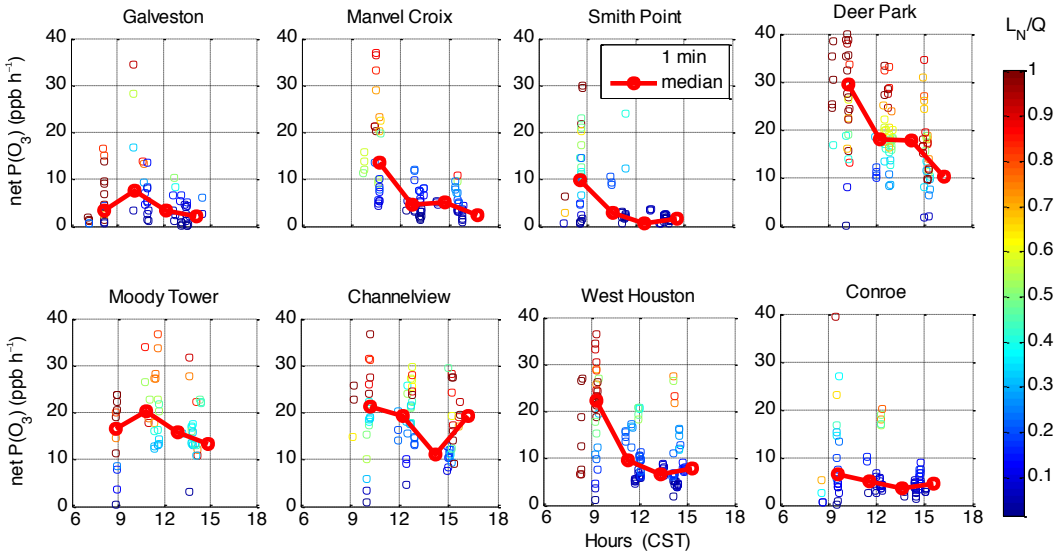

Figure 9. Diurnal variations of ozone production rate at eight individual spiral locations. Individual points are 1 min data colored with L_N/Q and the linked red circles represent the median values in hourly bins of $P(O_3)$. Data are limited with the pressure altitude less than 1000 m to represent the lowest layer of the atmosphere.

Figure 12 shows the photochemical oxidant O_x as a function of NO_z during DISCOVER-AQ in Houston in 2013. The two data sets plotted here were collected on 25 and 26 September, when high ambient ozone concentrations were observed, and for the data collected during all other flights. Note that the slopes obtained from these two data sets are essentially the same and an average OPE of ~8 is derived from the observations, meaning that 8 molecules of ozone were produced when one molecule of NO_x was consumed. Even though higher ozone concentrations were observed on 25 and 26 September, the OPEs on these 2 days are not different from those on other flights, indicating the ozone event on these 2 days was not caused by a higher OPE but mainly by higher concentrations of ozone precursors (and thus higher ozone production rates) and background ozone as indicated by the intercepts in the regression of the two data sets in Fig. 12. The high ozone observed on those days could also be due to slower ventilation and different meteorological conditions such as a lower boundary layer height, northerly transport from inland air pollution source regions, stagnant conditions from the high-pressure system, and the bay and gulf breezes.

The OPE value of ~8 during DISCOVER-AQ in Houston in 2013 is greater than the average OPE value obtained during the Texas Air Quality Study in 2006 (TexAQS 2006; OPE = 5.9 ± 1.2) (Neuman et al., 2009) and TexAQS 2000

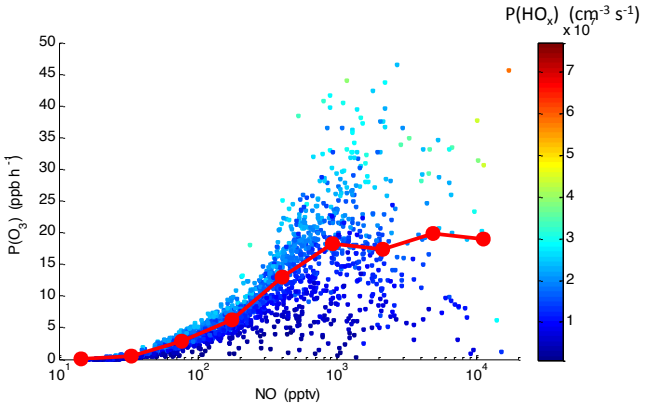

Figure 10. Ozone production as a function of NO mixing ratio. Individual data points are the 1 min averages and are colored with the production rate of HO_x ($= OH + HO_2$) during DISCOVER-AQ in Houston in 2013. The linked solid red circles represent the median values in [NO] bins. Note a log scale is used for the x axis.

(OPE = 5.4) (Ryerson et al., 2003). One possible reason for this increased OPE is that the continuous reduction in NO_x emissions in Houston from 2000 to 2013 pushed NO_x levels closer to 1 ppbv in 2013 (Fig. S1 in the Supplement); thus OPE increased since OPE increases as NO_x decreases when the NO_x level is greater than $\sim$ 1 ppbv (Fig. 13).

Houston area OPE values range from about a factor of 1.3 to 2 higher than the OPEs calculated from the DISCOVER-AQ 2011 study in Maryland, likely due to higher photochemical reactivity in Houston (Fig. S4). The 2011 Maryland OPEs ranged from 3.4 to 6.1 when all measured data below 1 km were used (Ren, X., unpublished data). An OPE of $\sim$ 8 was calculated (He et al., 2013) for the 2011 Maryland DISCOVER-AQ campaign for measured data below the 850 hPa level during vertical spirals with a strong linear correlation ($r^2 > 0.8$) between O_x and NO_z. Additionally, OPEs of 7.7–9.7 were obtained from a ground site during the New England Air Quality Study (NEAQS) 2002 (Griffin et al., 2004).

When calculating ozone production efficiency using observed O_x and NO_z, it is important to know whether there is substantial loss of nitric acid (HNO_3), because it can affect the OPE by reducing the NO_z (Trainer et al., 1993, 2000; Neuman et al., 2009) and thus bias the OPE high. The derived OPE in Fig. 12 is only valid when there is minimum loss of NO_z (especially HNO_3) from the source region to the point of observations. Neuman et al. (2009) found that $\Delta CO / \Delta NO_y$, i.e., the slope in a CO vs. NO_y plot, is an indicator for distinguishing plumes with efficient O_3 formation from plumes with similarly high O_3-to-NO_x oxidation product correlation slopes caused by variable mixing of aged polluted air depleted in HNO_3. A typical $\Delta CO / \Delta NO_y$ ranges from $\sim$ 40 in background air to $\sim$ 4–7 in fresh emission plumes in Houston (Neuman et al., 2009). The $\Delta CO / \Delta NO_y$ was examined at different times of the day on September 25 and 26. The results indicate that the $\Delta CO / \Delta NO_y$ was about 6.2 (Fig. 14a) throughout the day with variation between 6.0 and 7.0 (Fig. 14). This demonstrates that the observed O_3 formation was from fresh plumes and was not caused by variable mixing of aged polluted air depleted in HNO_3.

Using both the box model and CMAQ model results, OPE can also be calculated according to its definition, i.e., the net ozone formation rate divided by the formation rate of NO_z. Net $P(O_3)$ was calculated using Eq. (1), while the NO_z formation rate is the sum of HNO_3 and organic nitrate formation rates. The agreement between the box-model-derived and the CMAQ-derived OPEs is very good, with the mean OPEs of 14.8 ± 7.4 in the box model and 16.6 ± 8.1 in the CMAQ model. The dependence of OPE on NO_x is also similar for both the box and CMAQ models (Fig. 13). On average, the maximum of OPE appears at a NO_x level around 1 ppbv. In general, if the NO_x level is below 1 ppbv, OPE increases as the NO_x level increases, while if the NO_x level is above 1 ppbv, OPE decreases as the NO_x level increases (Fig. 13).

The OPE values calculated using the CMAQ and box model are greater than the values derived from the observations using the slope in the scatterplot of O_x vs. NO_z in Fig. 12. This is expected because, in the calculation of OPE using the box and CMAQ model results, a few ozone loss processes, such as ozone dry deposition and horizontal/vertical dispersion, were not considered. This could result in higher calculated ozone production rates when using the model results.

Spatial variations of OPE demonstrate that, except for a few hot spots over downtown Houston and the Houston Ship Channel, most large OPEs appear away from the urban center, e.g., the northwest and southeast of the area, while in areas with high NO_x emissions close to the urban center lower OPEs were generally observed (Fig. 15). This is again consistent with the results in Fig. 13 that the maximum of OPE appears at a NO_x level around 1 ppbv.

4 Discussion and conclusions

On average, $P(O_3)$ was about 20–30 ppbv h^{-1} in the morning and 5–10 ppbv h^{-1} in the afternoon during DISCOVER-AQ in Houston in 2013. The diurnal variation of $P(O_3)$ shows a broad peak in the morning with significant $P(O_3)$ in the afternoon obtained on 10 flight days in September 2013. High $P(O_3)$ mainly occurred with L_N/Q greater than 0.5, i.e., in the VOC-sensitive regime. Since $P(O_3)$ depends on NO_x levels and radical production rate, it increases as [NO] increases up to $\sim$ 1 ppbv and then levels off with further increases of [NO]. At a given [NO], a higher production rate of HO_x results in a higher ozone production rate. This has implications for the NO_x control strategies in order to achieve the ozone control goal.

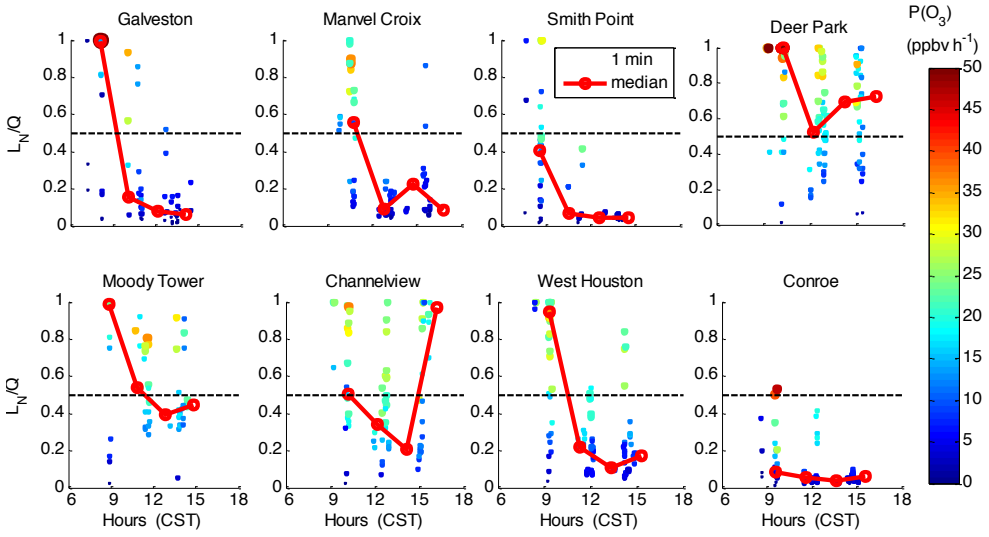

Figure 11. Diurnal variations of the indicator of ozone production sensitivity to NO_x and VOCs, L_N/Q, at eight individual spiral locations during DISCOVER-AQ in Houston in 2013. Individual points are 1 min data colored by $P(O_3)$, and the linked red circles represent the median values in hourly bins of $P(O_3)$. Data are limited with the pressure altitude less than 1000 m to represent the lowest layer of the atmosphere.

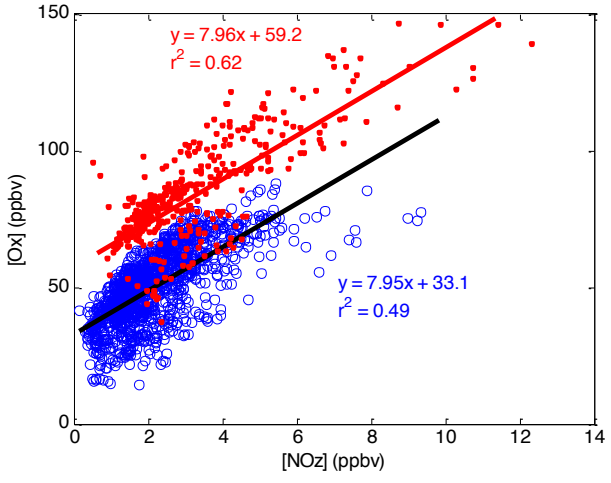

Figure 12. Photochemical oxidant, O_x $(=O_3+NO_2)$, as a function of NO_z $(=NO_y-NO_x)$ during DISCOVER-AQ in Houston in 2013. Red dots are the data collected on 25 and 26 September 2013, when high ambient ozone concentrations were observed. Blue circles are the data collected during other flights. Data are limited with the pressure altitude less than 1000 m to represent the lowest layer of the atmosphere.

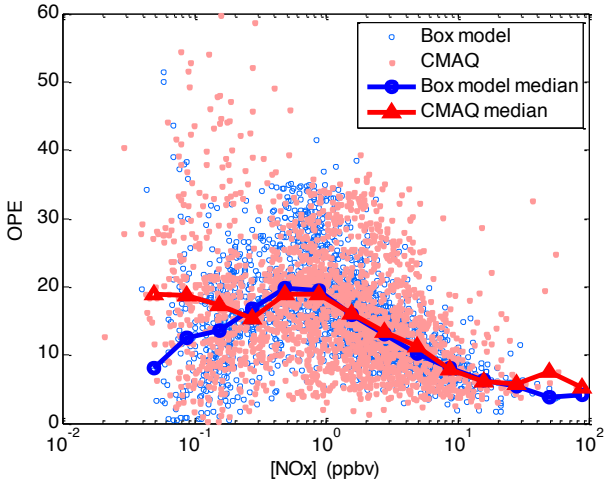

Figure 13. Ozone production efficiency (OPE) vs. NO_x in the box model (blue circles) and CMAQ model (pink dots) results. The linked blue circles show the median OPE values binned by NO_x concentration in the box model, while the linked red triangles show the median OPE values binned by NO_x concentration in the CMAQ model; OPE is calculated according to its definition as the net ozone formation rate divided by of the formation rate of NO_z.

The DISCOVER-AQ campaign in Houston is unique because of its large spatial coverage and thus spatial variations of ozone production and its sensitivity to NO_x and VOCs. Diurnal variations of $P(O_3)$ at eight individual locations where the P-3B conducted vertical spirals show that the $P(O_3)$ is on average more than 10 ppbv h^{-1} at locations with high NO_x and VOC emissions, such as Deer Park, Moody Tower, and Channelview, while at locations away from the urban center with lower emissions of ozone precursors such as Galveston, Smith Point, and Conroe, the ozone production rate is usually less than 10 ppbv h^{-1} on average. Hot spots of $P(O_3)$ were observed over downtown Houston and the Houston Ship Channel due to significant emissions in these areas.

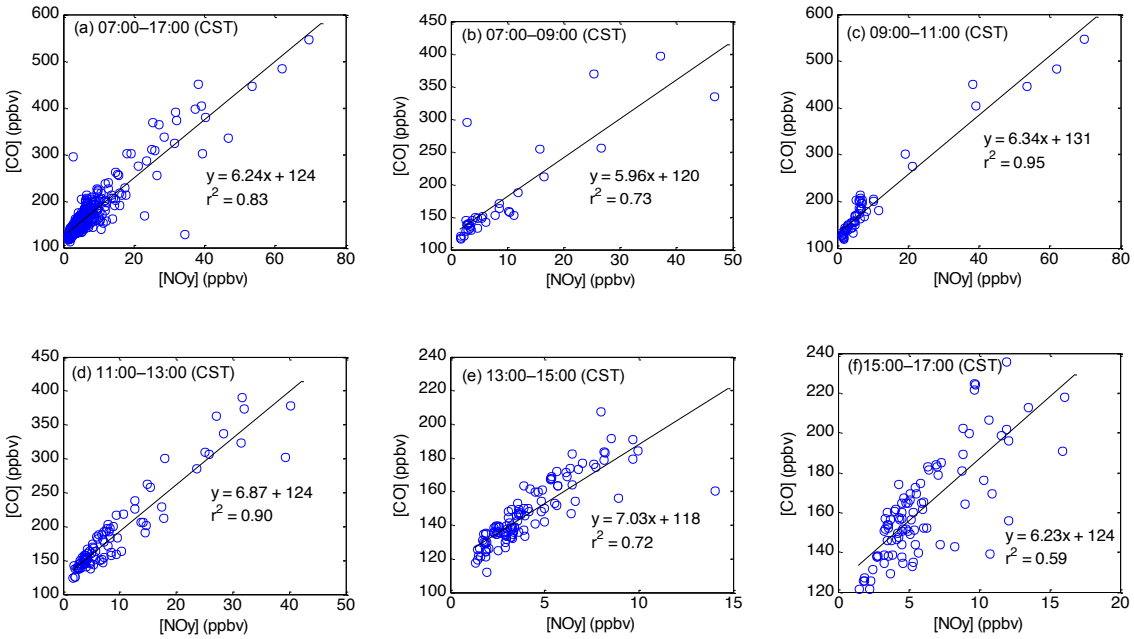

Figure 14. CO vs. NO_y and linear regression on 25 and 26 September at different times of the day: **(a)** 07:00–17:00 CST (all data), **(b)** 07:00–09:00 CST, **(c)** 09:00–11:00 CST, **(d)** 11:00–13:00 CST, **(e)** 13:00–15:00 CST, and **(f)** 15:00–17:00 CST.

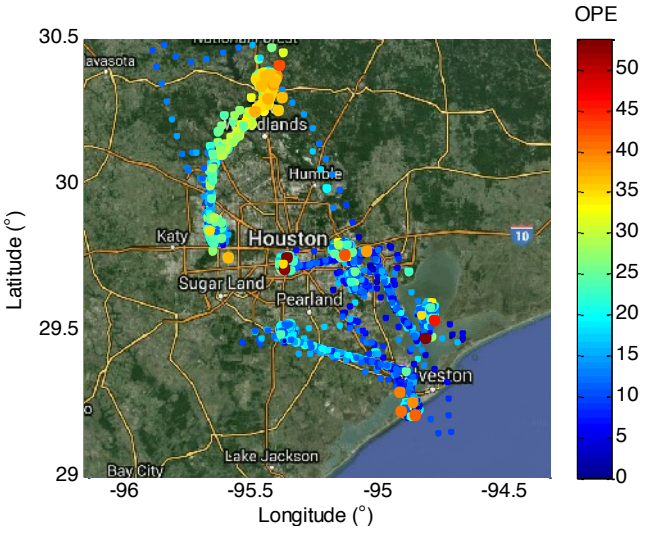

Figure 15. Ozone production efficiency along the P-3B flight track during DISCOVER-AQ in Houston in 2013. OPE was calculated using the box model results as the ratio of net ozone formation rate to the formation rate of NO_z.

Ozone production tended more towards VOC-sensitive in the morning with high $P(O_3)$ and, in general, NO_x-sensitive in the afternoon with some exceptions. It was found that, during some afternoon time periods and locations, $P(O_3)$ was VOC-sensitive. The diurnal variation of L_N/Q indicates that $P(O_3)$ was mainly VOC-sensitive in the early morning and then transitioned towards the NO_x-sensitive regime later in the day. High $P(O_3)$ in the morning was mainly associated with VOC sensitivity due to high NO_x levels in the morning. Specifically, Deer Park was mostly VOC-sensitive for the entire day, Moody Tower and Channelview were VOC-sensitive or in the transition regime, and Smith Point and Conroe were mostly NO_x-sensitive for the entire day.

Based on the measurements on the P-3B, OPE was about 8 during DISCOVER-AQ 2013 in Houston. This OPE value is greater than the average OPE value (5.9 ± 1.2) obtained during TexAQS 2006, likely due to the reduction in NO_x emissions in Houston between 2006 and 2013 that pushed NO_x levels closer to 1 ppbv in 2013 from higher NO_x levels in previous years. The results from this work strengthen our understanding of O_3 production; they indicate that controlling NO_x emissions will provide air quality benefits over the greater Houston metropolitan area in the long run, and in selected areas controlling VOC emissions will also be beneficial.

5 Data availability

One-minute averaged aircraft data during DISCOVER-AQ in Houston in 2013 that were used to constrained the box model were obtained from the the NASA DISCOVER-AQ data archive at http://www-air.larc.nasa.gov/missions/discover-aq/discover-aq.html. The box and CMAQ model output data are available upon request; please contact X. Ren (ren@umd.edu).

The Supplement related to this article is available online at doi:10.5194/acp-16-14463-2016-supplement.

Acknowledgements. The authors acknowledge the entire DISCOVER-AQ science team for the use of the P-3B measurement data in this work as well as Winston Luke and Paul Kelley at NOAA Air Resources Laboratory for helpful discussion. This work was funded by the Texas Commission on Environmental Quality (TCEQ) through the Air Quality Research Program (AQRP) at University of Texas Austin (contract no. 14-020) and a NASA ACMAP grant (grant no. NNX15AE31G). The contents, findings, opinions, and conclusions are the work of the authors and do not necessarily represent the findings, opinions, or conclusions of the TCEQ or AQRP. NASA AQAST supported Russell R. Dickerson.

Edited by: A. Carlton
Reviewed by: two anonymous referees

References

Appel, K. W., Gilliam, R. C., Pleim, J. E., Pouliot, G. A., Wong, D. C., Hogrefe, C., Roselle, S. J., and Mathur, R.: Improvements to the WRF-CMAQ modeling system for fine-scale air quality simulations, EM, 16–21 2014.

Canty, T. P., Hembeck, L., Vinciguerra, T. P., Anderson, D. C., Goldberg, D. L., Carpenter, S. F., Allen, D. J., Loughner, C. P., Salawitch, R. J., and Dickerson, R. R.: Ozone and NO_x chemistry in the eastern US: evaluation of CMAQ/CB05 with satellite (OMI) data, Atmos. Chem. Phys., 15, 10965–10982, doi:10.5194/acp-15-10965-2015, 2015.

Chen, S., Ren, X., Mao J., Chen, Z., Brune, W. H., Lefer, B., Rappenglück, B., Flynn J., Olson, J., and Crawford, J. H.: A comparison of chemical mechanisms based on TRAMP–2006 field data, Atmos. Environ., 44, 4116–4125, 2010.

DISCOVER-AQ whitepaper, http://discover-aq.larc.nasa.gov/pdf/DISCOVER-AQ_science.pdf, 2009.

Finlayson-Pitts, B. J. and Pitts, J.: Chemistry of the upper and lower atmosphere: Theory, experiments and applications, Academic Press, San Diego, California, 264–276, 2000.

Goldberg, D. L., Vinciguerra, T. P., Anderson, D. C., Hembeck, L., Canty, T. P., Salawitch, R. J., and Dickerson, R. R.: CAMx Ozone Source Attribution in the Eastern United States using Guidance from Observations during DISCOVER-AQ Maryland, Geophys. Res. Lett., 43, 2249–2258, doi:10.1002/2015GL067332, 2016.

Griffin, R. J., Johnson, C. A., Talbot, R. W., Mao, H., Russo, R. S., Zhou, Y., and Sive B. C.: Quantification of ozoneformation metrics at Thompson Farm during the New England Air Quality Study (NEAQS) 2002, J. Geophys. Res., 109, D24302, doi:10.1029/2004JD005344, 2004.

He, H., Hembeck, L., Hosley, K. M., Canty, T. P., Salawitch, R. J., and Dickerson, R. R.: High ozone concentrations on hot days: The role of electric power demand and NO_x emissions, Geophys. Res. Lett., 40, 5291–5294, 2013.

Jacob, D. J.: Introduction to Atmospheric Chemistry, Princeton University Press, New Jersey, 1999.

Kleinman, L. I., Daum, P. H., Lee, Y.-N, Nunnermacker, L. J., Springston, S. R., Weinstein-Lloyd J., and Rudolph, J.: Sensitivity of ozone production rate to ozone precursors, Geophys. Res. Lett., 28, 2903–2906, 2001.

Kleinman, L. I., Daum, P. H., Lee, Y.-N., Nunnermacker, L. J., Springston, S. R., Weinstein-Lloyd, J., and Rudolph, J.: Ozone production efficiency in an urban area, J. Geophys. Res., 107, 4733, doi:10.1029/2002JD002529, 2002.

Kleinman, L. I., Daum, P. H., Lee, Y.-N., Nunnermacker, L. J., Springston, S. R., Weinstein-Lloyd, J., and Rudolph, J.: A comparative study of ozone production in five US metropolitan areas, J. Geophys. Res., 110, D02301, doi:10.1029/2004JD005096, 2005a.

Kleinman, L. I.: The dependence of tropospheric ozone production rate on ozone precursors, Atmos. Environ., 39, 575–586, 2005b.

Lei, W., Zhang, R., Tie, X., and Hess, P.: Chemical characterization of ozone formation in the Houston-Galveston area: A chemical transport model study, J. Geophys. Res., 109, D12301, doi:10.1029/2003JD004219, 2004.

Li, G., Zhang, R., Fan, J., and Tie, X.: Impacts of biogenic emissions on photochemical ozone production in Houston, Texas, J. Geophys. Res., 112, D10309, doi:10.1029/2006JD007924, 2007.

Mallet, V. and Sportisse, B.: A comprehensive study of ozone sensitivity with respect to emissions over Europe with a chemistry-transport model, J. Geophys. Res., 110, D22302, doi:10.1029/2005JD006234, 2005.

Mao, J., Ren, X., Chen, S., Brune, W. H., Chen, Z., Martinez, M., Harder, H., Lefer, B., Rappenglück, B., Flynn, J., and Leuchner, M.: Atmospheric oxidation capacity in the summer of Houston 2006: Comparison with summer measurements in other metropolitan studies, Atmos. Environ., 44, 4107–4115, 2010.

Molina, M. J. and Molina, L. T.: Megacities and atmospheric pollution, J. Air Waste Manage., 54, 644–680, 2004.

Neuman, J. A., Nowak, J. B., Zheng, W., Flocke, F., Ryerson, T. B., Trainer, M., Holloway, J. S., Parrish, D. D., Frost, G. J., Peischl, J., Atlas, E. L., Bahreini, R., Wollny, A. G., and Fehsenfeld, F. C.: Relationship between photochemical ozone production and NO_x oxidation in Houston, Texas, J. Geophys. Res., 114, D00F08, doi:10.1029/2008JD011688, 2009.

Ren, X., van Duin, D., Cazorla, M., Chen, S., Mao, J., Zhang, L., Brune, W. H., Flynn, J. H., Grossberg, N., Lefer, B. L., Rappenglück, B., Wong, K. W., Tsai, C., Stutz, J., Dibb, J. E., Jobson, B. T., Luke, W. T., and Kelley, P.: Atmospheric oxidation chemistry and ozone production: Results from SHARP 2009 in Houston, Texas, J. Geophys. Res., 118, 5770–5780, 2013.

Ryerson, T. B., Trainer, M., Angevine, W. M., Brock, C. A., Dissly, R. W., Fehsenfeld, F .C., Frost, G. J., Goldan, P. D., Holloway, J. S., Hubler, G., Jakoubek, R. O., Kuster, W. C., Neuman, J. A., Nicks, D. K., Parrish, D. D., Roberts, J. M., Sueper, D. T., Atlas, E. L., Donnelly, S. G., Flocke, F., Fried, A., Potter, W. T., Schauffler, S., Stroud, V., Weinheimer, A. J., Wert, B. P., Wiedinmyer, C., Alvarez, R. J., Banta, R. M., Darby, L. S., and Senff, C. J.: Effect of petrochemical industrial emissions of reactive alkenes and NO_x on tropospheric ozoneformation in Houston, Texas, J. Geophys. Res., 108, 4249, doi:10.1029/2002JD003070, 2003.

Sillman, S.: The use of NO_y, H_2O_2, and HNO_3 as indicators for O_3-NO_x-hydrocarbon sensitivity in urban locations, J. Geophys. Res., 100, 14175–14188, 1995.

Sillman, S., Vautard, R., Menut, L., and Kley, D.: O_3-NO_x-VOC sensitivity and NO_x-VOC indicators in Paris: Results from models and Atmospheric Pollution Over the Paris Area (ESQUIF) measurements, J. Geophys. Res., 108, 8563, doi:10.1029/2002JD001561, 2003.

Tang, X., Wang, Z., Zhu, J., Gbaguidi, A. E., Wu, Q., Li, J., and Zhu, T., Sensitivity of ozone to precursor emissions in urban Beijing with a Monte Carlo scheme, Atmos. Environ., 44, 3833–3842, 2010.

Thielmann, A., Prévôt, A. S. H., and Staehelin, J.: Sensitivity of ozone production derived from field measurements in theItalian Po basin, J. Geophys. Res., 107, 8194, doi:10.1029/2000JD000119, 2002.

Trainer, M., Parrish, D. D., Buhr, M. P., Norton, R. B., Fehsenfeld, F. C., Anlauf, K. G., Bottenheim, J. W., Tang, Y. Z., Wiebe, H. A., Roberts, J. M., Tanner, R. L., Newman, L., Bowersox, V. C., Meagher, J. F., Olszyna, K. J., Rodgers, M. O., Wang, T., Berresheim, H., Demerjian, K. L., and Roychowdhury, U. K.: Correlation of ozone with NO_y in photochemically aged air, J. Geophys. Res., 98, 2917–2925, 1993.

Trainer, M., Parrish, D. D., Goldan, P. D., Roberts, J., and Fehsenfeld, F. C.: Review of observation-based analysis of the regional factors influencing ozone concentrations, Atmos. Environ., 34, 2045–2061, 2000.

Xue, L. K., Wang, T., Gao, J., Ding, A. J., Zhou, X. H., Blake, D. R., Wang, X. F., Saunders, S. M., Fan, S. J., Zuo, H. C., Zhang, Q. Z., and Wang, W. X.: Ozone production in four major cities of China: sensitivity to ozone precursors and heterogeneous processes, Atmos. Chem. Phys. Discuss., 13, 27243–27285, doi:10.5194/acpd-13-27243-2013, 2013.

Yarwood, G., Rao, S., Yocke, M., and Whitten, G. Z.: Updates to the Carbon Bond Mechanism: CB05, Final Report to the US EPA (RT-0400675), http://www.camx.com/publ/pdfs/CB05_Final_Report_120805.pdf, 2005.

Zaveri, R. A., Berkowitz, C. M., Kleinman, L. I., Springston, S. R., Doskey, P. V., Lonneman, W. A., and Spicer, C. W.: Ozone production efficiency and NO_x depletion in an urban plume: Interpretation of field observations and implications for evaluating O_3-NO_x-VOC sensitivity, J. Geophys. Res., 108, 4436, doi:10.1029/2002JD003144, 2003.